

# Ligand Effects on the Kinetics of the Reversible Binding of NO to Selected Aminocarboxylato Complexes of Iron(II) in Aqueous Solution

Thorsten Schnepfensieper,<sup>[a]</sup> Alicja Wanat,<sup>[a,b]</sup> Grazyna Stochel,<sup>\*,[a]</sup> Sara Goldstein,<sup>[c]</sup> Dan Meyerstein,<sup>[d]</sup> and Rudi van Eldik<sup>\*,[a]</sup>

**Keywords:** Catalysts / Chelates / Iron / Kinetics / Nitrogen oxides

Rate constants for the formation and dissociation of  $\text{Fe}^{\text{II}}(\text{L})\text{NO}$  ( $\text{L}$  = aminocarboxylato) have been determined using stopped-flow, temperature jump, flash photolysis, and pulse radiolysis techniques. For a series of ligands the formation rate constants vary between  $1.6 \times 10^6$  and  $2.4 \times 10^8 \text{ M}^{-1} \text{ s}^{-1}$ , whereas the dissociation rate constants vary between 0.11 and  $3.2 \times 10^3 \text{ s}^{-1}$  at 25 °C. These rate constants result in

stability constants ( $K_{\text{NO}} = k_f/k_d$ ) ranging from  $5.0 \times 10^2$  to  $1.1 \times 10^7 \text{ M}^{-1}$ , which are in good agreement with values of  $K_{\text{NO}}$  determined by a combined spectrophotometric and potentiometric technique. The results are discussed with reference to available literature data, and interpreted in terms of a generalized reaction mechanism.

## Introduction

It has been our interest in recent years to find metal chelates for the selective and efficient binding of NO in aqueous solution, to be employed in alternative denitrification processes.<sup>[1]</sup> Metal ions can catalyse such processes and can also increase the degree of absorption of NO by direct coordination to the metal center.<sup>[2,3]</sup> The fundamental coordination chemistry involves the reversible or partially reversible binding of NO by inexpensive and highly soluble metal complexes. Aminocarboxylato complexes of iron(II) are known for their ability to bind NO rapidly,<sup>[4–7]</sup> and are therefore used to enhance the solubility of NO in aqueous solution in industrial applications, in order to remove NO from exhaust gases. Little mechanistic information is presently available on these reactions, although some scattered rate constants for these reactions and stability constants are reported in the literature.<sup>[8–20]</sup>

In a recent systematic study<sup>[1]</sup> we reported the extent to which the reversible binding of NO to aminocarboxylato complexes of iron(II) can be tuned by the selected chelate. In general, a good correlation between the oxygen sensitivity of the chelated iron(II) complex and the formation constant for the  $\text{Fe}^{\text{II}}(\text{L})\text{NO}$  complex, i.e. the ability of chelated iron(II) to bind NO was found. This trend correlated with

a decreasing reversibility of the reaction, i.e. the ability of  $\text{Fe}^{\text{II}}(\text{L})\text{NO}$  to release NO, and an increasing tendency of  $\text{Fe}^{\text{II}}(\text{L})\text{NO}$  to exist as  $\text{Fe}^{\text{III}}(\text{L})\text{NO}^-$  in solution. The latter complex underwent subsequent slow decomposition, during which  $\text{Fe}^{\text{III}}(\text{L})$  and  $\text{N}_2\text{O}$  were formed.

We have now performed systematic kinetic studies on the reaction of NO with selected  $\text{Fe}^{\text{II}}$  complexes, based on their rather unique behaviour as observed in our more general and qualitative investigation referred to above.<sup>[1]</sup> These include  $\text{Fe}^{\text{II}}$  complexes of edta, hedtra, nta, dtpa, ttha, and mida (see Table 1 for selected abbreviations). Of this series, the  $\text{Fe}^{\text{II}}$ mida and  $\text{Fe}^{\text{II}}$ edta complexes behave totally differently with respect to the binding of NO. The  $\text{Fe}^{\text{II}}$ mida complex shows almost no oxygen sensitivity, exhibits a low binding affinity for NO, and releases NO almost completely when an inert gas was passed through the solution. In contrast,  $\text{Fe}^{\text{II}}$ edta is extremely oxygen-sensitive, shows a very high binding affinity for NO, and releases NO slowly and incomplete when treated with an inert gas. Kinetic studies on the formation and dissociation reactions were performed using complementary stopped-flow, temperature jump, flash photolysis, and pulse radiolysis techniques. The results are compared to available data for some of these systems reported in the literature. Our studies provide a quantitative basis for the earlier observed trends and reveal important mechanistic information.

## Results and Discussion

### Employed Kinetic Techniques

It was the purpose of this study to clarify the basic kinetics of the binding of NO to a series of aminocarboxylato complexes of iron(II). Table 2 summarizes the available kinetic and thermodynamic data on such reactions using a variety of techniques.<sup>[4]</sup> In many cases the reported rate constants were determined in an indirect manner, which re-

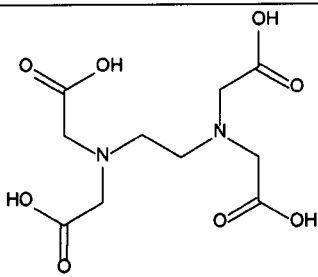
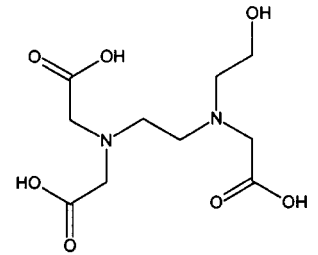
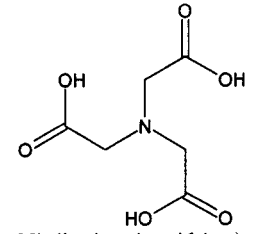
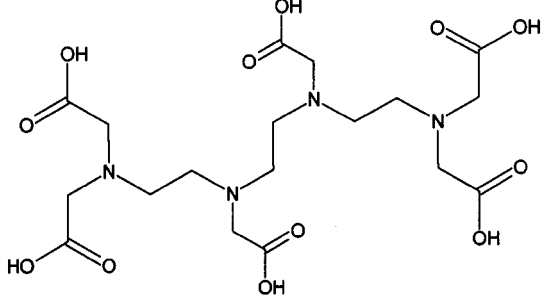
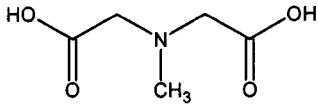
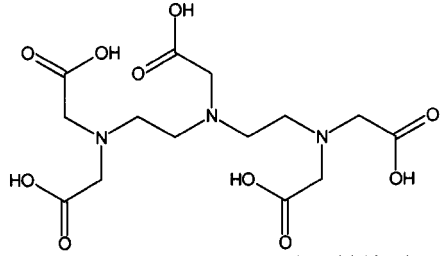
<sup>[a]</sup> Institute for Inorganic Chemistry, University of Erlangen-Nürnberg, Egerlandstraße 1, 91058 Erlangen, Germany  
Fax: (internat.) + 49-(0)9131/85-27387  
E-mail: vaneldik@chemie.uni-erlangen.de

<sup>[b]</sup> Department of Inorganic Chemistry, Jagiellonian University, Ingardena 3, 30-060 Krakow, Poland  
Fax: (internat.) + 48-12/633-5392  
E-mail: stochel@chemia.uj.edu.pl

<sup>[c]</sup> Department of Physical Chemistry, The Hebrew University of Jerusalem, Jerusalem 91904, Israel

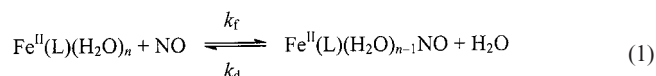
<sup>[d]</sup> Chemistry Department, Ben-Gurion University of the Negev, Beer-Sheva, and The College of Judea and Samaria, Ariel, Israel

Table 1. Summary of the chelate ligands used in this study

Structure Name (Abbreviation)
 <p>Ethylenediaminetetraacetic acid (edta)</p>
 <p>Hydroxyethylenediaminetriacetic acid (Hedtra)</p>
 <p>Nitrilotriacetic acid (nta)</p>
 <p>Triethylenetetraminehexaacetic acid (ttha)</p>
 <p>Methyliminodiacetic acid (mida)</p>
 <p>Diethylenetriaminepentaacetic acid (dtpa)</p>

sulted in large variations in the reported data. In order to verify the earlier data and obtain data on new systems, we employed different complementary kinetic techniques (for more details see Exp. Sect.).

The binding of NO to  $\text{Fe}^{\text{II}}(\text{L})$  can be expressed by the overall reaction shown in Equation (1). Different kinetic techniques can be used to measure  $k_f$  and  $k_d$ .



Stopped-flow techniques can be employed to rapidly mix solutions containing the reactants if the reactions occur on the millisecond time scale. The observed rate constant in the presence of excess of  $\text{Fe}^{\text{II}}(\text{L})$  can be expressed as shown in Equation (2), from which  $k_f$  and  $k_d$  can be extracted by measuring  $k_{\text{obs}}$  as a function of  $[\text{Fe}^{\text{II}}(\text{L})]$ . The ratio  $k_f/k_d$  equals the overall equilibrium constant  $K_{\text{NO}}$ , and should be in agreement with values for  $K_{\text{NO}}$  determined in other non-kinetic ways. A combination of UV/Vis spectroscopy and electrochemical detection of NO was used to determine  $K_{\text{NO}}$ , which was found to range from  $(1.0 \pm 0.1) \times 10^3$  to  $(1.5 \pm 0.2) \times 10^7 \text{ M}^{-1}$  at 25 °C for the series of complexes investigated.<sup>[1]</sup>

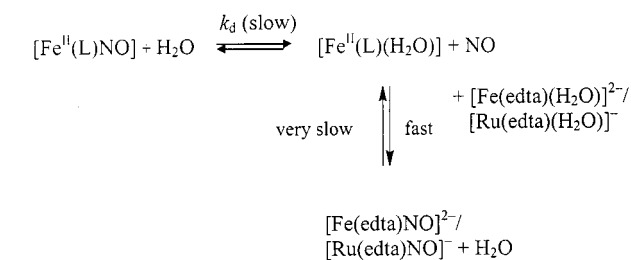
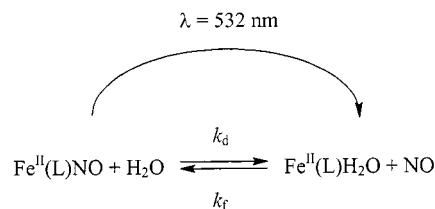
$$k_{\text{obs}} = k_f[\text{Fe}^{\text{II}}(\text{L})] + k_d \quad (2)$$

In principle it is also possible to measure  $k_d$  directly, and not by the determination of an intercept according to Equation (2), by using an NO-trapping technique with the stopped-flow method. In this case  $\text{Fe}^{\text{II}}(\text{L})\text{NO}$  is treated with another complex that binds NO more strongly and rapidly than the system under investigation. Under such condition, release of NO can become the rate-limiting step, which means that  $k_d$  can be determined directly from the observed kinetic trace. Two suitable complexes for determining  $k_d$  for the release of NO from  $\text{Fe}^{\text{II}}(\text{L})\text{NO}$  are  $\text{Fe}^{\text{II}}(\text{edta})(\text{H}_2\text{O})^{2-}$  (excluding L = edta) and  $\text{Ru}^{\text{III}}(\text{edta})\text{H}_2\text{O}^-$ , both of which react rapidly ( $k_f$  is ca.  $1 \times 10^8 \text{ M}^{-1} \text{ s}^{-1}$  at pH = 5 and 25 °C)<sup>[4,21]</sup> with NO to form the corresponding nitrosyl complexes (see Scheme 1). When an excess of either of these complexes is employed, such that the release of NO, i.e.  $k_d$ , becomes the rate-limiting step, the observed rate constant becomes independent of the excess concentration employed and equals  $k_d$ .

Flash photolysis can be employed to study the kinetics of Equation (1) on a significantly faster time scale. Irradiation at 532 nm induces the release of NO, followed by relaxation kinetics to the original equilibrium position (see Scheme 2), for which the rate expression of Equation (2) applies.

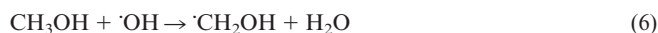
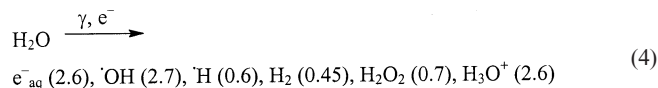
A third kinetic technique employed in this study is temperature jump. This technique can be used to perturb changes in the equilibrium position for systems that exhibit a significant temperature dependence. For the observed relaxation kinetics, the first-order rate constant is given by

Complex	pH	$T$ [K]	$k_f$ [ $\text{M}^{-1} \text{s}^{-1}$ ]	$k_d$ [ $\text{s}^{-1}$ ]	$K_{\text{NO}}$ [ $\text{M}^{-1}$ ]	Ref.
$\text{Fe}^{\text{II}}(\text{edta})$	4.6–8.0	298	$1.7 \times 10^8$		$1.5 \times 10^6$	[8]
	7.6	313			$1.5 \times 10^6$	[8]
	3.0	311			$3.5 \times 10^6$	[9]
	3.0	328			$8.6 \times 10^5$	[9]
	3.0	343			$3.4 \times 10^5$	[9]
	1.5–2.5	298	$(3.3 \pm 0.2) \times 10^7$			[10]
	7.0	298	$(1.2 \pm 0.1) \times 10^8$			[10]
	9.5–10	298	$(1.0 \pm 0.1) \times 10^8$			[10]
	5.1	298	$> 6.0 \times 10^7$	$> 60$		[2]
	6.0–8.0	308			$9.9 \times 10^6$	[11]
	2.5–11.0	298	$9.4 \times 10^7$		$3.1 \times 10^6$	[12]
	7.0	298	$1.2 \times 10^8$			[13]
	7.0	313	$1.4 \times 10^8$			[13]
	7.0	333	$1.4 \times 10^8$			[13]
	7.0	353	$1.5 \times 10^8$			[13]
	—	288			$2.2 \times 10^6$	[14]
	—	298			$1.5 \times 10^6$	[14]
	—	308			$7.8 \times 10^5$	[14]
	—	328			$5.3 \times 10^5$	[14]
	—	348			$2.5 \times 10^5$	[14]
	—	293			$1.7 \times 10^6$	[15]
	—	313			$3.9 \times 10^5$	[15]
	—	333			$1.1 \times 10^5$	[15]
$\text{Fe}^{\text{II}}(\text{dtpa})$	5.0	298	$(2.7 \pm 0.2) \times 10^5$	$< 23 \pm 11$	$> 1.2 \times 10^4$	[5]
$\text{Fe}^{\text{II}}(\text{nta})$	—	295			$5.9 \times 10^5$	[16]
	—	313			$3.0 \times 10^5$	[16]
	—	333			$1.0 \times 10^5$	[16]
	4.5–9.0	298	$1.6 \times 10^7$		$3.3 \times 10^6$	[12]
	5.0–7.0	298	$> 7.1 \times 10^7$	$> 35$	$> 2 \times 10^6$	[17]
	5.5	313			$(8.7 \pm 0.2) \times 10^5$	[17]
	5.5	323			$(4.6 \pm 0.2) \times 10^5$	[17]
	5.5	333			$(2.5 \pm 0.2) \times 10^5$	[17]
	4.0–9.0	293			$1.8 \times 10^6$	[18]
	4.0–9.0	313			$7.7 \times 10^5$	[18]
	4.0–9.0	333			$2.2 \times 10^5$	[18]
	< 1.0	298	$6.2 \times 10^5$	$1.4 \times 10^3$	$4.5 \times 10^2$	[19]
$\text{Fe}^{\text{II}}(\text{H}_2\text{O})_6$	2.0	298	$8.7 \times 10^5$	$2.3 \times 10^3$	$3.8 \times 10^2$	[20]
	< 1.0	298	$(7.1 \pm 1.0) \times 10^5$	$(1.5 \pm 0.6) \times 10^3$	$(4.7 \pm 2.0) \times 10^2$	[2]


$$k_{\text{obs}} = 1/\tau = k_{\text{f}}\{\text{Fe}^{\text{II}}(\text{L})(\text{H}_2\text{O})\}_{\text{e}} + [\text{NO}]_{\text{e}}\} + k_{\text{d}} \quad (3)$$


A fourth kinetic technique employed in this study is pulse radiolysis. The reaction of  $\text{Fe}^{\text{II}}(\text{L})$  with NO was studied by pulse-irradiation of aqueous solutions containing 2 mM  $\text{Fe}^{\text{III}}(\text{L})$ , 58–170  $\mu\text{M}$  NO, 1 M methanol, and either 2 mM acetate or phosphate buffer. Under these conditions,  $\text{e}_{\text{aq}}^-$  reduces  $\text{Fe}^{\text{III}}(\text{L})$  to  $\text{Fe}^{\text{II}}(\text{L})$  and  $\cdot\text{OH}$  is scavenged by  $\text{CH}_3\text{OH}$  to produce  $\cdot\text{CH}_2\text{OH}$  as shown in Equations (4) to (6). (The numbers in parenthesis are  $G$  values, which represent the

number of molecules formed per 100 eV energy absorbed by pure water.<sup>[22]</sup>



The  $\cdot\text{H}$  radicals are only a small fraction (ca. 10%) of the total radicals formed by the radiation, and most of them are scavenged by  $\text{CH}_3\text{OH}$  to produce  $\cdot\text{CH}_2\text{OH}$ , while the rest react with  $\text{NO}$ .<sup>[22]</sup> The reaction rate of  $\text{NO}$  with  $\cdot\text{CH}_2\text{OH}$  is expected to be similar to that with ethanol radical, i.e.  $3 \times 10^9 \text{ M}^{-1} \text{ s}^{-1}$ ,<sup>[22]</sup> most probably forming  $\text{O}=\text{N}-\text{CH}_2\text{OH}$  as the primary product, which might further react to form  $\text{HO}-\text{N}=\text{CH}_2$ . The rate constant for the reaction of  $\text{Fe}^{\text{II}}\text{L}$  with  $\text{NO}$  was determined by monitoring the formation of the absorbance at 440 or 450 nm under pseudo-first-order conditions, where  $[\text{Fe}^{\text{II}}\text{L}] = \text{dose} \times G_e \approx 5 \mu\text{M}$  and  $[\text{NO}] \approx [\text{NO}]_0 - \text{dose} \times G_{\text{OH}} \approx 53-165 \mu\text{M}$ .

#### Data Measured for $k_f$ and $k_d$

##### Stopped-Flow Measurements

Recently,<sup>[23]</sup>  $k_f$  was measured directly using the stopped-flow technique, in the case of  $\text{Ru}^{\text{III}}(\text{edta})\text{H}_2\text{O}^-$  to be  $1 \times 10^7 \text{ M}^{-1} \text{ s}^{-1}$  in phosphate buffer at  $\text{pH} = 7.4$  and  $7.3^\circ\text{C}$ . In order to measure such high rate constants, second-order reaction conditions and low concentrations of both reactants were selected to obtain conditions where the reaction is slower than the dead time (2–4 ms) of the stopped-flow instrument. We repeated the measurements on the  $\text{Ru}^{\text{III}}(\text{edta})\text{H}_2\text{O}^-$  system in acetate buffer at  $\text{pH} = 5.0$  and  $8^\circ\text{C}$ ,<sup>[21]</sup> but surprisingly found  $k_f = 1 \times 10^5 \text{ M}^{-1} \text{ s}^{-1}$ , which is ca. 100 times slower than the literature value.<sup>[23]</sup> This apparent discrepancy could be resolved by considering that the buffer should not be present in the  $\text{Ru}^{\text{III}}$  solution, but only in the  $\text{NO}$ -containing solution prior to mixing in the stopped-flow instrument. The buffer can substitute the labile water molecule in  $\text{Ru}^{\text{III}}(\text{edta})\text{H}_2\text{O}^-$  and cause a much slower substitution reaction with  $\text{NO}$  in producing the final product  $\text{Ru}^{\text{II}}(\text{edta})(\text{NO}^+)^-$ . It follows from these measurements that the literature value is valid at  $8^\circ\text{C}$ , and a reason-

able extrapolation to  $25^\circ\text{C}$  results in  $k_f \approx 1 \times 10^8 \text{ M}^{-1} \text{ s}^{-1}$ . Similar experiments with  $\text{Fe}^{\text{II}}(\text{edta})$  and  $\text{Fe}^{\text{II}}(\text{hedtra})$  at low temperature and low reactant concentrations revealed that  $k_f$  for these complexes is on the limit or faster than  $5 \times 10^7 \text{ M}^{-1} \text{ s}^{-1}$  at  $\text{pH} = 5$  and  $25^\circ\text{C}$ , i.e. very similar to that reported for  $\text{Ru}^{\text{III}}(\text{edta})\text{H}_2\text{O}^-$ , and could not be resolved using this kinetic technique. The high  $k_f$  values make these complexes ideal candidates for studying the reverse release of  $\text{NO}$  on complexes that bind  $\text{NO}$  less rapidly, using the trapping technique referred to above. Alternatively, an excess of such a complex can be used to study the release of  $\text{NO}$  from a complex that exhibits a similar reactivity towards  $\text{NO}$ , since the concentration ratio then determines the nature of the final product and the extent to which the rate-determining release of  $\text{NO}$  will be observed.

For the systems under the current investigation,  $k_f$  could not be determined using stopped-flow techniques, even under low temperature and concentration conditions, and therefore flash photolysis, pulse radiolysis, and temperature jump techniques were employed. However, for all the investigated systems,  $k_d$  could be measured directly using either  $\text{Ru}^{\text{III}}(\text{edta})\text{H}_2\text{O}^-$  and/or  $\text{Fe}^{\text{II}}(\text{edta})\text{H}_2\text{O}^{2-}$  to trap  $\text{NO}$  as described below.

With  $\text{Fe}^{\text{II}}(\text{edta})\text{H}_2\text{O}^{2-}$  as the  $\text{NO}$  scavenger during the release of  $\text{NO}$  from  $\text{Fe}^{\text{II}}(\text{mida})\text{NO}$ , the absorption maximum at 444 nm, which is characteristic for  $\text{Fe}^{\text{II}}(\text{mida})\text{NO}$ ,

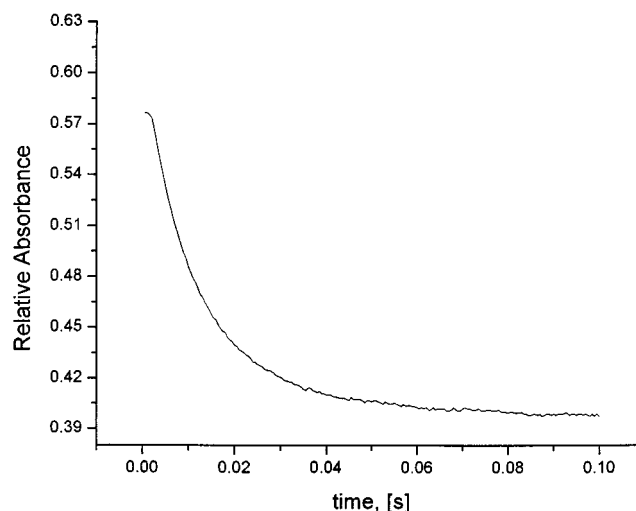


Figure 1. Typical absorbance-time plot for the release of  $\text{NO}$  from  $0.25 \text{ mM Fe}^{\text{II}}(\text{edta})\text{NO}_2^-$ , recorded with the stopped-flow instrument using  $7.5 \text{ mM Ru}^{\text{III}}(\text{edta})\text{H}_2\text{O}^-$  as a scavenger at  $\text{pH} = 5.0$  ( $0.05 \text{ M NaAc}$ ),  $\lambda = 436 \text{ nm}$ ,  $T = 24.4^\circ\text{C}$

Table 3. Dependence of  $k_d$  on  $[\text{Fe}^{\text{II}}(\text{edta})\text{H}_2\text{O}^{2-}]$  and  $[\text{Ru}^{\text{III}}(\text{edta})\text{H}_2\text{O}^-]$  in the presence of  $0.2 \text{ M}$  acetate buffer [ $\text{pH} = 5.0$ ;  $I = 0.5 \text{ M}$  ( $\text{NaClO}_4$ ),  $T = 25^\circ\text{C}$ ] for the release of  $\text{NO}$  from  $\text{Fe}^{\text{II}}(\text{mida})_2\text{NO}_2^-$

$1.5 \times 10^{-3} \text{ M Fe}^{\text{II}}(\text{mida})_2\text{NO}_2^- + x \text{ M Fe}^{\text{II}}(\text{edta})\text{H}_2\text{O}^{2-}$		$2.5 \times 10^{-3} \text{ M Fe}^{\text{II}}(\text{mida})_2\text{NO}_2^- + x \text{ M Ru}^{\text{III}}(\text{edta})\text{H}_2\text{O}^-$	
$[\text{Fe}^{\text{II}}(\text{edta})(\text{H}_2\text{O})^{2-}] [\text{M}]$	$k_d [\text{s}^{-1}]$	$[\text{Ru}^{\text{III}}(\text{edta})(\text{H}_2\text{O})^-] [\text{M}]$	$k_d [\text{s}^{-1}]$
$1.0 \times 10^{-3}$	$55.0 \pm 0.4$	$5.0 \times 10^{-3}$	$53.0 \pm 0.5$
$1.5 \times 10^{-3}$	$60.0 \pm 0.5$	$7.5 \times 10^{-3}$	$54.0 \pm 0.3$
$2.5 \times 10^{-3}$	$57.3 \pm 0.4$	$1.0 \times 10^{-2}$	$52.5 \pm 0.3$

decreased in intensity while a new band at 435 nm appeared, indicating the formation of  $\text{Fe}^{\text{II}}(\text{edta})\text{NO}^{2-}$ . The rate constant for NO release from  $\text{Fe}^{\text{II}}(\text{mida})\text{NO}$  was found

Table 4. Dependence of  $k_d$  for the release of NO from  $\text{Fe}^{\text{II}}(\text{edta})\text{NO}^{2-}$  on  $[\text{Ru}^{\text{III}}(\text{edta})\text{H}_2\text{O}^-]$  in the presence of 0.2 M acetate buffer [pH = 5.0;  $I = 0.5 \text{ M}$  ( $\text{NaClO}_4$ ),  $T = 25 \text{ }^\circ\text{C}$ ]

$2.5 \times 10^{-4} \text{ M Fe}(\text{edta})^{-2} + x \text{ M Ru}(\text{edta})\text{H}_2\text{O}^-$ [ $\text{Ru}(\text{edta})(\text{H}_2\text{O})^-$ ] [M]	$k_d$ [ $\text{s}^{-1}$ ]
$2.5 \times 10^{-3}$	$91.0 \pm 0.4$
$5.0 \times 10^{-3}$	$90.4 \pm 0.6$
$7.5 \times 10^{-3}$	$91.8 \pm 0.6$

to be  $57.3 \pm 0.4 \text{ s}^{-1}$  in the presence of excess of  $\text{Fe}^{\text{II}}(\text{edta})\text{H}_2\text{O}^{2-}$  and  $52.5 \pm 0.3 \text{ s}^{-1}$  in the presence of excess of  $\text{Ru}^{\text{III}}(\text{edta})\text{H}_2\text{O}^-$  at  $25 \text{ }^\circ\text{C}$ . Thus, there is a good agreement between the values of  $k_d$  determined using the two different NO scavengers. In both cases the rate-limiting step is the release of NO from the nitrosyl complex.

The release of NO from  $\text{Fe}^{\text{II}}(\text{edta})\text{NO}^{2-}$  with  $\text{Ru}^{\text{III}}(\text{edta})\text{H}_2\text{O}^-$  as a scavenger was complete within 100 ms, and  $k_d$  was calculated to be  $91.0 \pm 0.4 \text{ s}^{-1}$  at  $25 \text{ }^\circ\text{C}$ . A typical stopped-flow trace for this reaction is shown in Figure 1. The decrease in the absorption at 436 nm is consistent with the reaction equilibrium presented in Scheme 1. The observed rate constants were found to be independent of the concentration of the trapping complex as shown in

Table 5. Summary of kinetic data determined during this study for the reaction of NO with aminocarboxylato complexes of iron(II) at  $25 \text{ }^\circ\text{C}$

Complex	pH	$k_f$ [ $\text{M}^{-1}\text{s}^{-1}$ ]	$k_d$ [ $\text{s}^{-1}$ ]	$K_{\text{NO}} (= k_f/k_d)^{[\text{a}]}$ [ $\text{M}^{-1}$ ]	$K_{\text{NO}}$ [ $\text{M}^{-1}$ ]	Method
$\text{Fe}^{\text{II}}(\text{edta})$	4.9	$(1.5 \pm 0.2) \times 10^8$	$91.0 \pm 0.4$	$(2.1 \pm 0.5) \times 10^6$	$(2.1 \pm 0.2) \times 10^6$	pulse radiolysis
	7.2	$(1.7 \pm 0.4) \times 10^8$				flash photolysis
	5.0	$(2.4 \pm 0.1) \times 10^8$				stopped flow
	5.0					
$\text{Fe}^{\text{II}}(\text{hedtra})$	5.6	$(3.4 \pm 0.1) \times 10^7$	$4.2 \pm 0.1$	$(1.1 \pm 0.4) \times 10^7$	$(1.5 \pm 0.2) \times 10^7$	pulse radiolysis
	6.9	$(3.1 \pm 0.2) \times 10^7$				flash photolysis
	5.0	$(6.1 \pm 0.1) \times 10^7$				stopped flow
	5.0					
$\text{Fe}^{\text{II}}(\text{nta})$	3.5	$(1.2 \pm 0.1) \times 10^7$	$9.3 \pm 0.2$	$(1.8 \pm 0.5) \times 10^6$	$(1.8 \pm 0.2) \times 10^6$	pulse radiolysis
	5.4	$(1.3 \pm 0.1) \times 10^7$				flash photolysis
	6.8	$(1.4 \pm 0.1) \times 10^7$				stopped flow
	5.0	$(2.1 \pm 0.1) \times 10^7$				
	5.0					
$\text{Fe}^{\text{II}}(\text{dtpa})$	6.8	$(2.7 \pm 0.3) \times 10^5$	$5.5 \pm 0.4$	$(2.0 \pm 0.2) \times 10^6$	$(3.0 \pm 0.3) \times 10^6$	pulse radiolysis
	5.0	$(1.1 \pm 0.1) \times 10^7$				flash photolysis
	5.0					stopped flow
$\text{Fe}^{\text{II}}_2(\text{ttha})$	5.2	$(6.5 \pm 0.7) \times 10^5$	$0.11 \pm 0.01$	$(3.1 \pm 0.3) \times 10^7$	$(3.0 \pm 1.0) \times 10^7$	pulse radiolysis
	5.0	$(3.5 \pm 0.1) \times 10^6$				flash photolysis
	5.0					stopped flow
$\text{Fe}^{\text{II}}(\text{ttha})$	5.2	$(3.0 \pm 0.7) \times 10^5$	$0.39 \pm 0.01$	$(2.6 \pm 0.2) \times 10^6$	$(4.0 \pm 0.1) \times 10^6$	pulse radiolysis
	5.0	$(1.0 \pm 0.1) \times 10^6$				flash photolysis
	5.0					stopped flow
$\text{Fe}^{\text{II}}(\text{mida})$	5.0	$(1.9 \pm 0.1) \times 10^6$	$57.3 \pm 0.4$	$(2.1 \pm 0.6) \times 10^4$	$(9.5 \pm 0.7) \times 10^3$	flash photolysis
	5.0	$(8.5 \pm 2.4) \times 10^5$				temperature jump
	5.0					stopped flow
$\text{Fe}^{\text{II}}(\text{mida})_2$	5.0	$(1.8 \pm 0.1) \times 10^6$	$62.2 \pm 0.6$	$(2.9 \pm 0.2) \times 10^4$	$(2.2 \pm 0.6) \times 10^4$	flash photolysis
	5.0					stopped flow
$\text{Fe}^{\text{II}}(\text{H}_2\text{O})_6$	5.0	$(1.6 \pm 0.1) \times 10^6$	$(3.2 \pm 0.7) \times 10^3$ (from intercept) $788 \pm 100$ (at $5 \text{ }^\circ\text{C}$ )	$(5.0 \pm 1.4) \times 10^2$	$(1.2 \pm 0.1) \times 10^3$	flash photolysis
	5.0	(from slope)				stopped flow

<sup>[a]</sup> The stability constants were calculated from  $k_f/k_d$ , which were obtained kinetically. – <sup>[b]</sup> Stability constants for nitrosyl complexes are based on the equilibrium between  $\text{Fe}^{\text{II}}(\text{L})_x$  and  $\text{Fe}^{\text{II}}(\text{L})_x(\text{NO})$  complexes; the complex concentrations were measured using UV/Vis spectroscopy and the concentration of free NO in solution was determined directly with an NO electrode, from which  $K_{\text{NO}}$  was calculated.<sup>[1]</sup>



Tables 3 and 4, and therefore represent values for  $k_d$ . The results of these measurements are summarized in Table 5. The lowest  $k_d$  values were found for  $\text{Fe}^{\text{II}}(\text{ttha})\text{NO}^{4-}$  and  $\text{Fe}_2^{\text{II}}(\text{ttha})\text{NO}^{2-}$  with  $k_d = 0.39 \pm 0.01$  and  $0.11 \pm 0.01 \text{ s}^{-1}$  at 25 °C, respectively. The release of NO was found to be slightly faster for  $\text{Fe}^{\text{II}}(\text{hedtra})\text{NO}^-$  ( $k_d = 4.2 \pm 0.1 \text{ s}^{-1}$ ),  $\text{Fe}^{\text{II}}(\text{dtpa})\text{NO}^{3-}$  ( $k_d = 5.5 \pm 0.4 \text{ s}^{-1}$ ), and  $\text{Fe}^{\text{II}}(\text{nta})\text{NO}^-$  ( $k_d = 9.3 \pm 0.2 \text{ s}^{-1}$ ). Significantly higher rate constants were obtained for  $\text{Fe}^{\text{II}}(\text{mida})\text{NO}$  ( $k_d = 57.3 \pm 0.4 \text{ s}^{-1}$ ) and  $\text{Fe}^{\text{II}}(\text{mida})_2\text{NO}^{2-}$  ( $k_d = 62.2 \pm 0.6 \text{ s}^{-1}$ ), while the highest value was found for  $\text{Fe}^{\text{II}}(\text{edta})\text{NO}^{2-}$  ( $k_d = 91.0 \pm 0.4 \text{ s}^{-1}$ ). Kinetic data for the NO release in the case of edta, nta, and dtpa are available from the literature (see Table 2).<sup>[2,5,17]</sup> In the case of  $\text{Fe}^{\text{II}}(\text{edta})$  the predicted literature value of  $k_d > 60 \text{ s}^{-1}$  could be confirmed, whereas significantly lower rates were measured in the present study for nta and dtpa. The trapping technique employed enables a direct measurement of the dissociation rate constant, and in principle must give more accurate values than those obtained using indirect methods. By way of comparison,  $k_d$  for aquated iron(II) was found to be  $788 \pm 100 \text{ s}^{-1}$  (at 5 °C), i.e. aquated iron(II) binds NO very weakly and releases it rapidly. Extrapolated to 25 °C, the latter value is in good agreement with the value obtained from flash photolysis experiments (see further Discussion).

### Flash Photolysis Measurements

The procedure outlined in Scheme 2 was employed for all investigated systems. A typical kinetic trace is shown in Figure 2. The concentration dependence of  $k_{\text{obs}}$  resulted in linear plots, as predicted by Equation (2), for which typical examples are shown in Figures 3 and 4 for  $\text{Fe}^{\text{II}}(\text{nta})\text{NO}^-$  and  $\text{Fe}^{\text{II}}(\text{H}_2\text{O})_5\text{NO}^{2+}$ , respectively. The  $\text{Fe}^{\text{II}}(\text{edta})$  complex is the species with the highest formation rate constant, i.e.  $k_f = (2.4 \pm 0.1) \times 10^8 \text{ M}^{-1} \text{ s}^{-1}$  at 25 °C (pH = 5). This result agrees well with literature data (see Table 2), where rate constants around  $1.3 \times 10^8 \text{ M}^{-1} \text{ s}^{-1}$  at different pH values and temperatures were found. For  $\text{Fe}^{\text{II}}(\text{nta})$ ,  $\text{Fe}^{\text{II}}(\text{hedtra})$ , and  $\text{Fe}^{\text{II}}(\text{dtpa})$ ,  $k_f$  was found to be  $(2.1 \pm 0.1) \times 10^7$ ,  $(6.1 \pm 0.1) \times 10^7$  and  $(1.1 \pm 0.1) \times 10^7 \text{ M}^{-1} \text{ s}^{-1}$  at 25 °C, respectively. While the value for the nta system is in good agreement with data reported in the literature,<sup>[12]</sup> the obtained rate constant for the dtpa system is significantly higher than that obtained before with the temperature jump technique.<sup>[5]</sup> We believe, however, that the value measured in the present study is more reliable, since the stability constants ( $K_{\text{NO}}$ ) obtained from kinetic and thermodynamic measurements are in perfect agreement with these data (see Table 5). The  $\text{Fe}^{\text{II}}(\text{hedtra})$  complex reacts only half as fast as the edta complex, but the stability constant is more than five times higher, as a result of the NO release kinetics reported above. The  $k_f$  values for  $\text{Fe}_2^{\text{II}}(\text{ttha})$  and  $\text{Fe}^{\text{II}}(\text{ttha})$  are  $(3.5 \pm 0.1) \times 10^6$  and  $(1.0 \pm 0.1) \times 10^6 \text{ M}^{-1} \text{ s}^{-1}$  at 25 °C, respectively. The lowest  $k_f$  values were found for  $\text{Fe}^{\text{II}}(\text{mida})$

( $1.9 \times 10^6 \text{ M}^{-1} \text{ s}^{-1}$ ),  $\text{Fe}^{\text{II}}(\text{mida})_2$  ( $1.8 \times 10^6 \text{ M}^{-1} \text{ s}^{-1}$ ) and  $\text{Fe}^{\text{II}}(\text{H}_2\text{O})_6$  ( $1.6 \times 10^6 \text{ M}^{-1} \text{ s}^{-1}$ ), respectively.

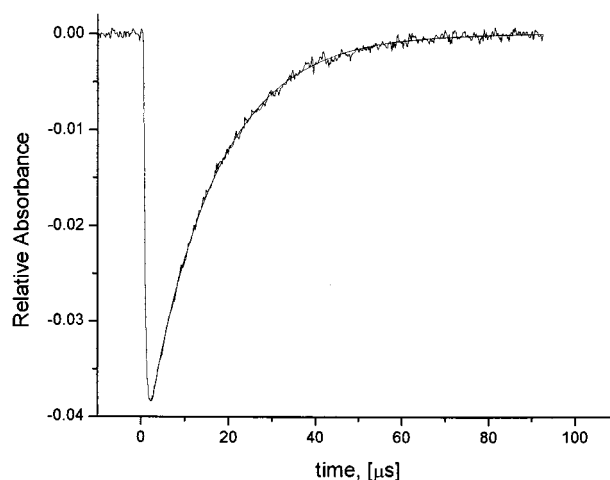


Figure 2. Typical absorbance-time plot for the reaction of  $\text{Fe}^{\text{II}}(\text{nta})$  with NO at pH = 5.0 (0.1 M NaAc),  $I = 0.5 \text{ M}$  ( $\text{NaClO}_4$ ) and  $T = 25 \text{ °C}$ ; photolysis wavelength = 532 nm, detection wavelength = 439 nm

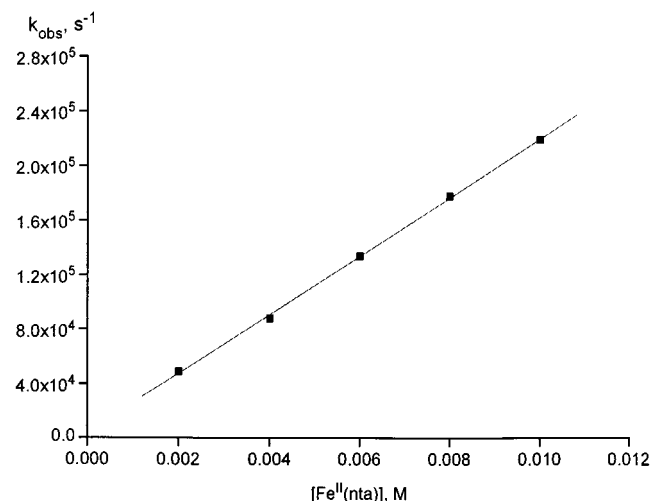


Figure 3. Plot of  $k_{\text{obs}}$  as a function of  $[\text{Fe}^{\text{II}}(\text{nta})]$ , measured at pH = 5.0 (0.2 M NaAc) and  $T = 25 \text{ °C}$ ; photolysis wavelength = 532 nm, detection wavelength = 439 nm

### Pulse Radiolysis Measurements

Figure 5 presents a typical absorbance-time trace recorded for the reaction of  $\text{Fe}^{\text{II}}(\text{edta})$  with NO using the pulse radiolysis procedure described above. Values of  $k_f$  determined with this method were slightly lower in comparison with the results obtained from the flash photolysis experiments, viz.  $1.5 \times 10^8 \text{ M}^{-1} \text{ s}^{-1}$  at pH = 4.9 for  $\text{Fe}^{\text{II}}(\text{edta})$ ,  $3.4 \times 10^7 \text{ M}^{-1} \text{ s}^{-1}$  at pH = 5.6 for  $\text{Fe}^{\text{II}}(\text{hedtra})$ , and  $1.3 \times 10^7 \text{ M}^{-1} \text{ s}^{-1}$  at pH = 5.4 for  $\text{Fe}^{\text{II}}(\text{nta})$ . This difference can probably be accounted for in terms of the different temperatures at which the experiments were performed, viz. ca. 20 °C in the pulse radiolysis experiments compared to 25 °C in the flash photolysis experiments. However, in the case of

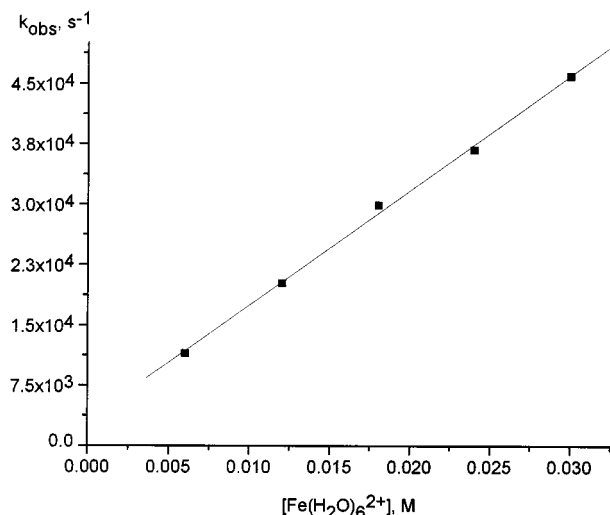


Figure 4. Plot of  $k_{\text{obs}}$  as a function of  $[\text{Fe}(\text{H}_2\text{O})_6^{2+}]$ , measured at pH = 5.0 (0.2 M NaAc) and  $T = 25^\circ\text{C}$ ; photolysis wavelength = 532 nm, detection wavelength = 451 nm

dtpa and ttha complexes (see Table 5), the values of  $k_f$  are much lower than those obtained in the flash photolysis experiments. For these systems it was not possible to perform a concentration dependence study due to the high absorbance of the 2 mM  $\text{Fe}^{\text{III}}(\text{L})$  solution. The second-order rate constant had to be calculated from a single point measured in the presence of 0.104 mM NO at 500 and 470 nm for the dtpa and ttha complexes, respectively. The absorbance changes at these wavelengths are extremely small, which further adds to the uncertainty in the rate constants. In addition, the calculated value of  $K_{\text{NO}}$  based on the rate constants from the flash photolysis experiments is in good agreement with the directly determined value. These facts lead us to conclude that the flash photolysis data probably

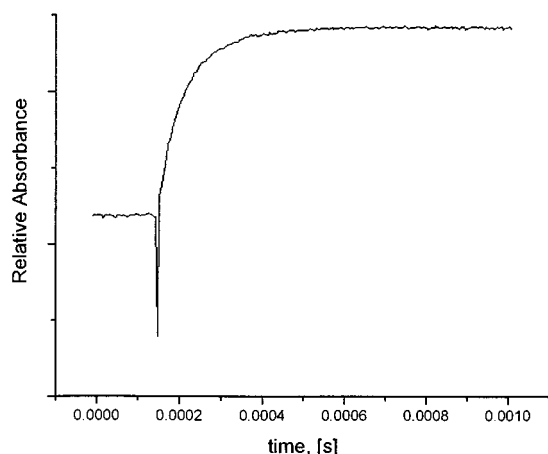


Figure 5. Typical absorbance-time trace for the reaction of  $\text{Fe}^{\text{II}}(\text{edta})\text{H}_2\text{O}_2^-$  with NO using pulse radiolysis; the solution contained 2 mM  $\text{Fe}^{\text{III}}(\text{edta})\text{H}_2\text{O}_2^-$ , 1 M  $\text{CH}_3\text{OH}$ , and 0.115 mM NO at pH = 7.2 (4 mM phosphate buffer), 1.5  $\mu\text{s}$  pulse duration,  $\lambda = 440\text{ nm}$ ,  $T = 20^\circ\text{C}$

represent the more realistic rate constants for the studied systems.

### Temperature Jump Measurements

Measurements of  $k_f$  for the  $\text{Fe}^{\text{II}}(\text{mida})$  complexes failed using pulse radiolysis. This led us to probe the temperature jump method to establish the accuracy of the data measured with the flash photolysis technique. Equilibrium mixtures of  $\text{Fe}^{\text{II}}(\text{mida})$  and  $\text{Fe}^{\text{II}}(\text{mida})\text{NO}$  were studied, and a typical absorbance-time trace is reported in Figure 6. A systematic concentration-dependence study according to Equation (3) (shown in Figure 7) resulted in  $k_f = (8.6 \pm 0.8) \times 10^5\text{ M}^{-1}\text{ s}^{-1}$ , which agrees within experimental errors with the data from the flash photolysis experiments. The intercept of the line represents  $k_d$  for the release of NO, and was found to be  $69 \pm 50\text{ s}^{-1}$ . Considering the large error limits (up to 15%) usually encountered in temperature jump

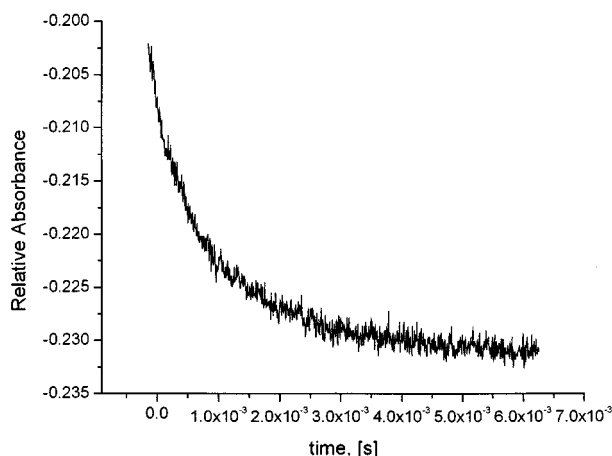


Figure 6. Typical absorbance-time trace for the reaction of  $\text{Fe}^{\text{II}}(\text{mida})$  with NO using the temperature jump techniques;  $k_{\text{obs}} = 1.08 \times 10^3\text{ M}^{-1}\text{ s}^{-1}$ ; experimental conditions:  $\lambda_{\text{det.}} = 444\text{ nm}$ ,  $T = 25^\circ\text{C}$ ,  $[\text{Fe}^{\text{II}}(\text{mida})\text{NO}] = 7.9 \times 10^{-4}\text{ M}$ ,  $[\text{Fe}^{\text{II}}(\text{mida})] = 1.2 \times 10^{-3}\text{ M}$ ,  $[\text{NO}] = 5.5 \times 10^{-5}\text{ M}$ , pH = 5.0 (0.1 M NaAc),  $I = 0.5$  ( $\text{NaClO}_4$ )

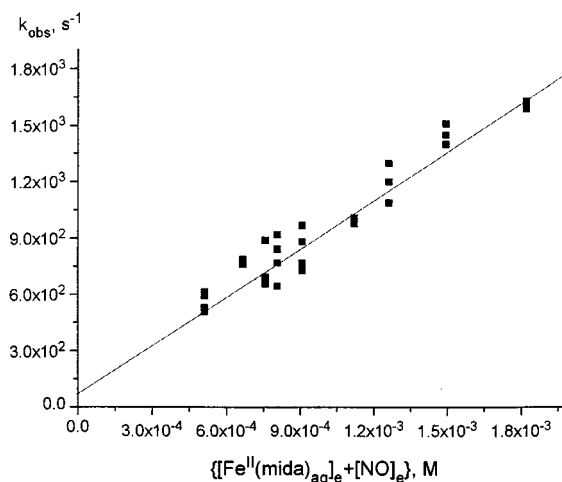


Figure 7. Plot of  $k_{\text{obs}}$  as a function of  $\{[\text{Fe}^{\text{II}}(\text{mida})_{\text{aq}}]_{\text{e}} + [\text{NO}]_{\text{e}}\}$  for the reaction of  $\text{Fe}^{\text{II}}(\text{mida})$  with NO obtained using the temperature jump technique; experimental conditions:  $\lambda_{\text{det.}} = 444\text{ nm}$ ,  $T = 25^\circ\text{C}$ , pH = 5.0 (0.1 M NaAc),  $I = 0.5$  ( $\text{NaClO}_4$ )

experiments, this value is in reasonable agreement with the more accurate one determined via stopped-flow measurements using the trapping technique.

## Conclusion

Four different kinetic techniques were employed to study the binding reaction of NO to a series of aminocarboxylato complexes of iron(II). Depending on the selected system, one or more techniques could be used to determine  $k_f$ . The rate constant for the dissociation of NO could be measured successfully in all cases using the stopped-flow technique and  $\text{Fe}^{\text{II}}(\text{edta})\text{H}_2\text{O}^{2-}$  or  $\text{Ru}^{\text{III}}(\text{edta})\text{H}_2\text{O}^-$  as NO scavengers. As a result of its higher stability and much less oxygen sensitivity,  $\text{Ru}^{\text{III}}(\text{edta})\text{H}_2\text{O}^-$  appears to be more promising for practical applications as an NO scavenger than  $\text{Fe}^{\text{II}}(\text{edta})\text{H}_2\text{O}^{2-}$ , although they both bind NO at approximately the same rate.

The fastest rate constant for the binding of NO was found in the case of edta, which is ca. 4 times faster than the reaction of  $\text{Fe}^{\text{II}}(\text{hedtra})\text{H}_2\text{O}$  with NO. Taking into account the 22 times faster NO release from the edta complex, the nitrosyl adduct of the hedta complex is around 5 times more stable than the edta complex at 25 °C. On this basis, we can account for the reported difference in the stability constants for these two complexes. The  $\text{Fe}^{\text{II}}(\text{nta})\text{NO}^-$  complex has approximately the same stability constant as the edta complex, where in this case both  $k_f$  and  $k_d$  are smaller. All other complexes have significantly lower stability constants due to their lower  $k_f$  values. On comparing the iron(II) complexes of mida and edta in terms of their application as catalysts for the exhaust gas denitrification, the reaction of  $\text{Fe}^{\text{II}}(\text{mida})$  with NO is approximately 100 times slower than the corresponding reaction with  $\text{Fe}^{\text{II}}(\text{edta})\text{H}_2\text{O}^{2-}$ , which accounts for almost the same difference in the value of  $K_{\text{NO}}$ . This apparent disadvantage of the mida complex could for example be partially compensated for by longer contact time between the exhaust gas and the catalyst. In addition, the mida complex is almost oxygen-insensitive, which prevents unwanted oxidation of the chelate and allows the effective regeneration of the catalyst.

In general, a good agreement between the values of  $K_{\text{NO}}$  calculated from the kinetic data and those determined directly with the aid of the NO electrode was observed (see Table 5). The thermodynamic value furthermore assisted the selection of appropriate kinetic data in those cases where differing  $k_f$  values were found. The results in Table 5 demonstrate the large influence of the aminocarboxylato chelates on the values of the rate constant and the overall equilibrium constant. There seems to be no simple correlation between these constants and the selected donor groups or charge on the iron(II) complexes. The formation reaction must to some degree be controlled by the lability of the coordinated water molecules on the iron(II) centre, whereas the dissociation reaction is largely affected by the oxidation state of the metal centre, viz.  $\text{Fe}^{\text{II}}-\text{NO}$  or  $\text{Fe}^{\text{III}}-\text{NO}^-$  or  $\text{Fe}^{\text{I}}-\text{NO}^+$ . The distribution of charge density in the

$\text{Fe}-\text{NO}$  bond should depend on the donor properties of the selected chelate. Solomon et al.<sup>[24]</sup> have clearly shown that in the case of  $\text{Fe}^{\text{II}}(\text{edta})\text{NO}$ , the  $\text{Fe}-\text{NO}$  centre has an  $\text{Fe}^{\text{III}}-\text{NO}^-$  character.

Details on the intimate mechanism of these reactions cannot be obtained from rate constant measurements only. With the kinetic methods now well worked out to investigate these reactions, it has become possible to go a step further and to study the temperature and pressure dependence of the formation and dissociation reactions reported here. From these dependencies the activation parameters ( $\Delta H^\ddagger$ ,  $\Delta S^\ddagger$ , and  $\Delta V^\ddagger$ ) can be obtained and used to gain further insight into the intimate nature of the underlying reaction mechanisms. In addition, since it is reasonable to expect that  $k_f$  is controlled by the lability of coordinated water, the rate and activation parameters for the solvent exchange reactions on the selected iron(II) complexes should also be studied. These results and their mechanistic interpretation will be reported in a forthcoming paper.

## Experimental Section

### Materials and Methods

**Chemicals:** All chemicals were of analytical grade and were used as received. Solutions were prepared with distilled and purified water using a Milli-Q water purification system. The ligands mida and nta were supplied by Akzo Nobel. All other ligands and chemicals were purchased from Arcos Chimica, Fluka, Lancaster Synthesis, or Sigma-Aldrich with the highest available purity (at least 97%). NO gas, purchased from Messer Griesheim or Rießner Gase in a purity of at least 99.5 vol-%, was cleaned from trace amounts of higher nitrogen oxides like  $\text{N}_2\text{O}_3$  and  $\text{NO}_2$  by passing it through an Ascarite II column (NaOH on silica gel, Sigma-Aldrich). NO from a gas tank should not be used after six months following the date of its industrial preparation, since decomposition causes a drastic decrease in the purity of the gas. The decomposition is pressure-dependent, which led us to only use bottles filled with a maximum pressure of 20 bar, and resulted in a longer lifetime of the NO gas. All experiments were performed under strict exclusion of air oxygen. Buffer solutions were deaerated for extended periods (in general 1 min per mL solution) with pure  $\text{N}_2$  or Ar, or in some cases using freeze-thaw cycles under vacuum, in order to completely remove the dissolved dioxygen in solution, before they were brought in contact with  $\text{Fe}^{\text{II}}$  salts or nitric oxide.

**Measurements:** The pH was measured using a Mettler Delta 340 pH-meter. The reference electrode was filled with NaCl instead of KCl to prevent precipitation of  $\text{KClO}_4$ . UV/Vis spectra were recorded with a Cary 1G UV/Vis spectrophotometer from Varian using a 1-cm quartz cuvette directly attached to a round flask with a side gas connection. The determination of the stability constants was performed as described elsewhere.<sup>[1]</sup> The concentration of free NO was determined with an ISO-NOP electrode connected to an ISO-NO Mark II nitric oxide sensor from World Precision Instruments. The NO electrode consists of a membrane-covered anode that selectively oxidizes NO to  $\text{NO}_3^-$  ions. The resulting current is proportional to the concentration of NO in solution. The NO electrode was calibrated daily with fresh solutions of sodium nitrite and potassium iodide according to the method suggested by the manufacturers. The calibration factor nA/ $\mu\text{M}$  was determined with a linear fit program.



## Kinetic Measurements

**Laser Flash Photolysis:** Laser flash photolysis kinetic studies were carried out with the use of the LKS.60 Spectrometer from Applied Photophysics for detection and a Nd:YAG laser (SURLITE I – 10 Continuum) pump source operating in the second ( $\lambda_{\text{exc.}} = 532 \text{ nm}$ ) harmonic (245 mJ pulses with ca. 7-ns pulse widths). Spectral changes at appropriate wavelength were monitored using a 100-W Xenon arc lamp, monochromator, and photomultiplier tube PMT – 1P22. The absorbance reading was balanced to zero before the flash, and data were recorded with a digital storage oscilloscope DSO HP 54522A and then transferred to a computer for sequential analysis. Gas-tight quartz cuvettes were used throughout this study. The rate constant for the NO uptake reaction was detected around 435 nm, where a maximum in the UV/Vis spectrum is present. A stock solution of NO was prepared in a gas-tight syringe by degassing a 0.2 M acetate buffer solution (pH = 5.0), followed by saturation with NO. Dilutions of known concentration were prepared from this saturated solution by the use of the syringe technique. Oxygen-free solutions of iron(II) complexes were synthesized and diluted to appropriate concentrations in the vacuum line.

**Pulse Radiolysis:** Pulse radiolysis experiments were carried out with the Varian 7715 linear accelerator with 5-MeV electrons pulses of 0.5  $\mu\text{s}$  and 200 mA current. The dose per pulse was determined with the hexacyanoferrate(II) dosimeter [5 mM  $\text{K}_4\text{Fe}(\text{CN})_6$  in  $\text{N}_2\text{O}$ -saturated water] using  $G[\text{Fe}(\text{CN})_6^{3-}] = 6.7 \times 10^3 \text{ M}^{-1} \text{ cm}^{-1}$  at 420 nm<sup>[25]</sup> to be 13.8 Gy. A 150-W Xe lamp produced the analysing light. Appropriate filters were used to minimize photochemistry. Irradiation was carried out in a 4-cm Spectrosil cell using three light passes. Nitric oxide solutions were prepared in gas-tight syringes by purging first the water with He to remove  $\text{O}_2$ , followed by bubbling for 30 min with NO. NO-saturated solutions (1.8 mm at 21 °C and 690 Torr)<sup>[26]</sup> were stored in syringes and subsequently diluted with He-saturated solutions to the desired concentrations by the syringe technique.

**Temperature Jump:** The complex formation reactions were studied using the earlier described joule-heating temperature jump apparatus (rise time  $\approx 10 \mu\text{s}$ ) (Messanlagen, Göttingen)<sup>[27]</sup> A temperature jump of 3 °C was applied to solutions thermostatically maintained at 22 °C during an electric discharge of ca. 20 kV. Kinetic traces for relaxation were monitored mostly at 444 nm, with at least 5, and up to 10, replicate traces being processed as reported earlier,<sup>[28,29]</sup> by emulating a transient recorder with a 486 PC equipped with a TR-PC 25-8 card from Dr. Strauss System Elektronik GmbH. After the jump, a single relaxation process was observed in each trace. The rate constant for the relaxation curve was fitted with the OLIS KINFIT program.<sup>[30]</sup>

**Stopped-Flow:** The kinetics of NO release from  $\text{Fe}^{\text{II}}(\text{L})\text{NO}$  were studied with a thermostated ( $\pm 0.1 \text{ }^\circ\text{C}$ ) stopped-flow spectrometer (SX-18 MV, Applied Photophysics) coupled to an online data acquisition system. At least five kinetic runs were recorded under all conditions, and the reported rate constants represent the mean values. The kinetic data were analysed with the OLIS KINFIT program.

## Acknowledgments

T. S. and R. v. E. gratefully acknowledge financial support from Akzo Nobel Functional Chemicals, Paques Bio Systems, Fonds der Chemischen Industrie, and the Max-Buchner-Forschungsförderung.

Studies at the Jagiellonian University were supported by the State Committee for Scientific Research, Poland, KBN (3TO9A11515 and 1605/T09/2000/19) and the Foundation for Polish Science ("Fastkin" No. 8/97). D. M. acknowledges support from the Alexander von Humboldt Foundation.

- [1] T. Schnepfensieper, S. Finkler, A. Czap, R. van Eldik, M. Heus, P. Nieuwenhuizen, C. Wreesmann, W. Abma, *Eur. J. Inorg. Chem.* **2001**, 491–501.
- [2] D. Littlejohn, S.-G. Chang, *J. Phys. Chem.* **1982**, *86*, 537–540.
- [3] S.-G. Chang, D. Littlejohn, S. Lynn, *Environ. Prog. Technol.* **1983**, *17*, 649.
- [4] J. F. Demmink, I. C. F. van Gils, A. A. C. M. Beenackers, *Ind. Eng. Chem. Res.* **1997**, *36*, 4914–4927.
- [5] V. Zang, R. van Eldik, *Inorg. Chem.* **1990**, *29*, 4462–4468.
- [6] S. S. Tsai, S. A. Bedell, L. H. Kirby, D. J. Zabcik, *Environ. Prog.* **1989**, *8*, 126–129.
- [7] V. Zang, M. Kotowski, R. van Eldik, *Inorg. Chem.* **1988**, *27*, 3279.
- [8] M. Teramoto, S. –I. Hiramane, Y. Shimada, Y. Sugimoto, H. Teranishi, *J. Chem. Eng. Jpn.* **1978**, *11*, 450–457.
- [9] Y. Hishinuma, R. Kaji, H. Akimoto, F. Nakajima, T. Mori, T. Kamo, Y. Arikawa, S. Nozawa, *Bull. Chem. Soc. Jpn.* **1979**, *52*, 2863–2865.
- [10] E. Sada, H. Kumazawa, I. Kudo, T. Kondo, *Ind. Eng. Chem. Proc. Des. Dev.* **1980**, *19*, 377–382.
- [11] E. Sada, H. Kumazawa, Y. Takada, *Ind. Eng. Chem. Fundam.* **1984**, *23*, 60–64.
- [12] W. Weisweiler, R. Blumhofer, T. Westermann, *Chem. Eng. Proc.* **1986**, *20*, 155–166.
- [13] S.-M. Yih, C.-W. Lii, *Chem. Eng. Comm.* **1988**, *73*, 43–53.
- [14] L. Huasheng, F. Wenchi, *Ind. Eng. Chem. Res.* **1988**, *27*, 770–774.
- [15] H. Nymoen, D. van Velzen, H. Langenkamp, *Chem. Eng. Proc.* **1993**, *32*, 9–12.
- [16] J. Hofele, D. van Velzen, H. Langenkamp, K. Schaber, *Chem. Eng. Proc.* **1996**, *35*, 295–300.
- [17] N. Lin, D. Littlejohn, S.-G. Chang, *Ind. Chem. Proc. Des. Dev.* **1982**, *21*.
- [18] E. Sada, H. Kumazawa, H. Machida, *Ind. Eng. Chem. Res.* **1987**, *26*, 1468–1472.
- [19] K. Kustin, I. A. Taub, E. Weinstock, *Inorg. Chem.* **1996**, *5*, 1079–1082.
- [20] H. Hikita, S. Asai, H. Ishikawa, S. Hirano, *J. Chem. Eng. Jpn.* **1977**, *10*, 120–124.
- [21] T. Schnepfensieper, A. Wanat, G. Stochel, R. van Eldik, manuscript in preparation.
- [22] A. B. Ross, W. G. Mallard, W. P. Helman, J. V. Buxton, R. E. Huie, P. Neta *NIST Standard References Database 40, Version 2.0*, **1994**.
- [23] N. A. Davies, M. T. Wilson, E. Slade, S. P. Fricker, B. A. Murrer, N. A. Powell, G. R. Henderson, *Chem. Commun.* **1997**, 47–48.
- [24] C. A. Brown, M. A. Pavlosky, T. E. Westre, Y. Zhang, B. Hedman, K. O. Hodgson, E. I. Solomon, *J. Am. Chem. Soc.* **1995**, *117*, 715–732.
- [25] G. V. Buxton, C. R. Stuart, *J. Chem. Soc., Faraday Trans.* **1995**, *91*, 279.
- [26] *Lange's Handbook of Chemistry*, 13th ed. (Ed.: J. A. Dean), Mc Graw-Hill, New York, p. 10.
- [27] R. Doss, R. van Eldik, H. Kelm, *Rev. Sci. Instrum.* **1982**, *9*, 715.
- [28] D. H. Powell, A. E. Merbach, I. Fábíán, S. Schindler, R. van Eldik, *Inorg. Chem.* **1994**, *33*, 4468.
- [29] H. D. Projahn, S. Schindler, R. van Eldik, *Inorg. Chem.* **1995**, *3*, 5935.
- [30] OLIS KINFIT, Bogart, GA, USA.

Received January 30, 2001  
[I01038]